RSC Advances

Ru Doping Enhanced Resistive Switching Behavior in InGaZnO Thin Films

Journal:	*RSC Advances*
Manuscript ID	RA-ART-01-2016-002174.R1
Article Type:	Paper
Date Submitted by the Author:	08-Apr-2016

Complete List of Authors:	Li, Qin; Xi\'an Jiaotong University, State Key Laboratory for Mechanical Behavior of Materials Li, Yanhuai; Xi\'an Jiaotong University, State Key Laboratory for Mechanical Behavior of Materials Gao, Leiwen; Xi\'an Jiaotong University, State Key Laboratory for Mechanical Behavior of Materials Ma, Fei; Xi'an Jiaotong University, State Key Laboratory for Mechanical Behavior of Materials Song, Zhongxiao; Xi’an Jiaotong University, State Key Laboratory for Mechanical Behavior of Materials Xu, Kewei; Xi\'an Jiaotong University, State Key Laboratory for Mechanical Behavior of Materials; Xi’an University of Arts and Science, Department of Physics and Opt-electronic Engineering

Subject area & keyword:	Nanoscience - Physical < Physical

Ru Doping Enhanced Resistive Switching Behavior in InGaZnO Thin Films

Qin Li[1], Yanhuai Li[1], Leiwen Gao[1], Fei Ma[1,a)], Zhongxiao Song[1,a)], Kewei Xu[1,2]

[1]*State Key Laboratory for Mechanical Behavior of Materials, Xi'an Jiaotong University, Xi'an 710049, Shaanxi, China*

[2]*Department of Physics and Opt-electronic Engineering, Xi'an University of Arts and Science, Xi'an 710065, Shaanxi, China*

Abstract

In this paper, ruthenium (Ru) doped InGaZnO (IGZO:Ru) thin films were deposited by magnetron co-sputtering and the resistive switching behaviors were investigated. It was found that an appropriate Ru doping could weaken the bonding interaction between metal and oxygen atoms, facilitate the formation of robust conductive filaments, and enhance the electrical field locally, resulting in significantly enhanced bipolar resistive switching properties and a stable OFF/ON ratio of 10^5. But an excessive doping of Ru would accelerate the nucleation and formation of conductive filaments and, tiny and fragile conductive filaments were unexpectedly generated. In such a case, high resistive state was reached even no negative bias voltage was applied, resulting in volatile resistive behavior. A model was suggested to understand the effect of Ru doping on the properties of the thin films.

[a)] Authors to whom correspondence should be addressed.

Electronic mail: mafei@mail.xjtu.edu.cn; zhongxiaosong@mail.xjtu.edu.cn

1. Introduction

With the rapid development of information technology, nonvolatile memories (NVMs) with high-speed and large-capacity are urgently demanded. Resistive Random Access Memory (RRAM) is believed to be one of the most promising candidates for next nonvolatile memory, due to the simple structure, high operation speed and excellent scalability. Under an external bias voltage, a great many dielectric materials including perovskites, metal oxides and amorphous silicon, exhibit resistive switching (RS) characteristics[1,2]. Among these dielectric materials, transition metal oxides, such as, TiO_2, NiO, ZnO and HfO_x, as the most promising candidates for RRAM, have been extensively investigated.[3-6]

Because of the uniformity and stability, amorphous InGaZnO (a-IGZO) has attracted more and more attention in the field of RRAM in recent years.[7-11] In particular, if transparent a-IGZO memories can be combined with thin film transistors, they will have potential applications in system-on-panel displays.[10,11] However, lower switching ratio, higher power consumption and instability still restrict the application of a-IGZO in RRAM. Recently, many research works have been done to improve the performance of IGZO devices.[12-16] For examples, Wang et al.[12] adopted an arc-shaped bottom electrode to suppress the randomness of resistive switching process, and thus to improve the device uniformity and switching stability. Pei et al.[13] inserted thin SiO_2 layer between the top electrode and a-IGZO switching layer to improve the resistive switching characteristics as a result of reinforced electric field. Hu et al.[14] and Hwang

et al.[15] fabricated a-IGZO thin films by a low-temperature photochemical solution method and microwave irradiation technique, respectively. Both of them exhibited enhanced RRAM performance upon irradiation. It is well known that oxygen vacancies play an important role in resistive switching of transition metal oxide RRAMs,[16] and doping of Al[17], Cu[18], Co[19] and Au[20] could effectively modify the physical properties as well as the RRAM performance of oxide materials owing to the increased oxygen vacancies and trapping states. Nevertheless, to the best of our knowledge, the influence of doping on the RRAM performance of IGZO thin films has not been studied. It is worth noting that the doping of Ru in IGZO thin films might result in non-stoichiometric composition because Ru has more valence state as compared to the metals, In, Ga, Zn, in IGZO. Furthermore, the thermal stability of amorphous structure might be enhanced by heterogeneous atoms.[21] Hence, it is expected that the oxygen vacancies in IGZO thin films as well as the RRAM performance could be tuned through Ru doping. In this paper, we investigate the effects of Ru doping on the resistance switching properties of IGZO-based RRAM devices, and the physical mechanisms are discussed.

2. Experimental

Ru doped IGZO thin films with a thickness of 40 nm were deposited on Pt/Ti/SiO_2/Si substrates at room temperature by co-sputtering the targets of IGZO (99.99%, purity) and Ru (99.99%, purity) using radio frequency (RF) powers. The thickness of Pt and Ti layers were 125 nm and 25 nm, respectively. IGZO thin films

undoped with Ru atoms were deposited for comparison. Prior to the deposition, all the substrates were successively cleaned by ultrasonic treatment with alcohol, acetone, and deionized water to remove organic contaminants. A power of 80 W was applied on the IGZO target, but two powers of 20 W and 30 W on the Ru target, the samples are noted as 20W-Ru-IGZO and 30W-Ru-IGZO correspondingly. The stoichiometric ratio of In, Ga and Zn in the IGZO target was 1:1:1. During the sputtering, the working pressure was maintained at 0.3 Pa and the mixture of Ar and O_2 (4 vol.% O_2) was used as the sputtering gas. IGZO:Ru thin films 130 nm in thickness were deposited on Si substrates for microstructure characterization. Finally, Ag top electrodes (200 nm in thickness) with a diameter of 300 um were deposited on the devices under a direct current power of 70 W.

Glancing incident angle x-ray diffraction (XRD, XRD-7000) and cross-section high-resolution transmission electron microscopy (HR-TEM, JEM-2100F) were used to characterize the microstructures of the thin films. XRD patterns indicate that the as-deposited IGZO films are amorphous, no matter Ru doped or not. The cross-sectional HR-TEM images and the Inverse Fast Fourier Transform (IFFT) images show that the local atomic ordering in the 30W-Ru-IGZO sample changes as compared to the pure IGZO sample. The electrical properties were measured in dark by the Keithley 4200-SCS semiconductor analyzer in current-voltage (I-V) sweeping mode. During the I-V measurement, the Pt bottom electrode (BE) was grounded and the Ag top electrode (TE) was swept with a bias voltage. X-ray photoelectron

spectroscopy (XPS, ESCALAB 250Xi) was measured to analyze the chemical composition as well as the binding states in the medium layers by monochromatic Al Kα X-ray. It shows that the component of Ru in the as-deposited 20W-Ru-IGZO and 30W-Ru-IGZO samples is 0.7 at.% and 1.6 at.%, respectively.

3. Results and discussion

XPS were used to analyze the evolution of binding energies of atoms in IGZO-based films. To avoid the influence of adatom from the environment, the surface was etched by 4 nm using Ar^+ ions. As shown in Figures 1(a)-(c), the binding energies of indium (In $3d_{5/2}$), gallium (Ga $2p_{3/2}$) and zinc (Zn $2p_{3/2}$) in Ru doped IGZO red shift as compared to those in pure IGZO sample. It was reported that, in Co-doped In_2O_3, the binding energies of both In 3d and O 1s were lowered due to the smaller radius of Co^{2+}.[22] However, the binding energies of all the metals in IGZO films are lowered even for Ga ions with a smaller radius than that of Ru ions. In fact, if Zn atoms are substituted by Ru atoms, the distribution of oxygen vacancies and defects in ZnO will be modified.[23] Therefore, the red-shift in XPS peaks of metals should be mainly ascribed to the changes in bonding states between metals and oxygen. Furthermore, the formation energies of oxygen vacancies in In_2O_3, ZnO and Ga_2O_3 are 3.06 eV, 3.75 eV and 4.5 eV, respectively.[24,25] Comparatively, it is easier for In-O bonds to break, leading to the generation of oxygen vacancies and the largest shift of binding energy of In. Figure 1(d) shows the O1s XPS peaks of the samples. The O1s peaks are fitted into two sub-peaks at 530.5 eV (O_I) and 531.5 eV (O_{II}) by using a

Gaussian profile. The O_I peak is due to O^{2-} ions bonding with neighboring metals, while the O_{II} peak is associated with oxygen vacancies in the IGZO matrix[26-28]. Therefore, the O_{II}/O_I+O_{II} ratio could be adopted to evaluate the amount of oxygen vacancies. It can be observed from Figure 1(d) that the O_{II}/O_I+O_{II} ratio increases from 9.6% in pure IGZO, to 11.8% in 20W-Ru-IGZO and to 15.0% in 30W-Ru-IGZO samples, that is, the oxygen vacancies increase upon doping of Ru in IGZO thin films. Figure 1(e) shows the XPS spectra of Ru3d in 20W-Ru-IGZO and 30W-Ru-IGZO samples. However, it is difficult to identify the XPS peak of Ru3d5/2 in 20W-Ru-IGZO sample because of low doping concentration. Hence, the bonding states of Ru in IGZO thin films are deduced from the XPS spectra of Ru3d in the 30W-Ru-IGZO sample. Two sub-peaks at 279.8 eV and 281.5 eV correspond to Ru-Ru and Ru-O bonding states, indicating incomplete oxidation of Ru in the thin films and the existence of metallic clusters.

Figure 2(a) schematically displays the RRAM device and the cross-sectional TEM image of the thin film is shown in the inset. During I-V measurement, different compliance currents are exerted on the devices. As shown in Figure 2(b), bipolar resistance switching (BRS) characteristics are observed in the pure IGZO cell under compliance currents (CCs) of 100 mA and 0.1 mA after a forming process. Under a compliance current of 100 mA, the current increases abruptly at a set voltage of about 0.8 V as a result of switching from high-resistance state (HRS, OFF state) to low-resistance state (LRS, ON state). Subsequently, an opposite process switching

from ON state to OFF state could also be seen when the bias voltage is reversely swept to about -1 V. The resistance ratio of OFF and ON states (OFF/ON) is about 30 at a reading voltage of 0.1 V. Under a compliance current of 0.1 mA, the pure IGZO device also exhibits BRS properties with an extremely high OFF/ON ratio of about 10^5, but the device breaks down gradually after several cycles. However, the Ru-doped IGZO thin films exhibit a completely different performance as compared to pure IGZO samples. As shown in Figure 2(c), the 20W-Ru-IGZO thin films can be stably switched to ON state at a small CC of 0.1 mA, and stable bipolar resistance switching characteristics with a high resistance switching ratio of 10^5 are obtained, and the set voltage is about 0.5 V. As reported previously,[7-11] the set voltage of IGZO RRAMs was 1.5 V or above, and the compliance current was higher than 1 mA. Although ultraviolet and microwave irradiation could enhance the RS uniformity, the switching ratio (10-100 [14,15]) was still lower, and the set voltage (1-1.5 V [14,15]) was still higher, as compared to the results in this work. So Ru doping could effectively reduce the power consumption in IGZO RRAMs. Meanwhile, BRS can also be obtained under a CC of 1 mA within a few cycles. Fig 2(d) shows the endurance performance of 20W-Ru-IGZO devices under a CC of 0.1 mA. Apparently, the device exhibits excellent repeatability after 50 sweeping cycles, and the retention time is longer than 10^5 s without obvious resistance fluctuation, which is better than reported results of IGZO RRAMs.[7] But no repeatable bipolar resistive switching is observed in the 30W-Ru-IGZO samples no matter how large the CC is. Figure 2(e) as an example presents the resistance switching characteristics of the 30W-Ru-IGZO

thin films. Under a CC of 0.1 mA, the device switches to LRS at a positive voltage of about 0.6 V, but it recovers to HRS even before the negative bias is applied. Though BRS feature is evidenced at the CC of 1 mA, the curves fluctuate considerably during the repeated cycles. Figure 2(f) summarizes the electrical properties of the samples. It can be seen that the switching behaviors of Ag/IGZO:Ru/Pt devices are tunable by changing the compliance current and the concentration of doping Ru. Four resistive states are involved: (1) BRS, (2) BRS without endurance, (3) Volatile RS, and (4) Breakdown. “BRS without endurance” means that the resistance at LRS state fluctuates easily during cycling. “Volatile RS” indicates that the state degenerates easily once a negative bias is applied or even before the positive bias vanishes. “Breakdown” means that the thin films cannot reverse from LRS to HRS. Although both pure IGZO and 20W-Ru-IGZO samples manifest BRS characteristics, the level of CC is quite different: above 10 mA for pure IGZO, 0.1 mA - 5 mA for 20W-Ru-IGZO and a permanent breakdown will be induced when CC is above 5 mA. For 30W-Ru-IGZO sample, the switching properties are not stable and not controllable no matter how large the CC is.

To understand the conduction and switching mechanism of the memory devices, Figures 3(a) and (b) show the current-voltage (I-V) curves of pure IGZO and 20W-Ru-IGZO devices at positive bias voltage in double-logarithmic scale. They have a similar tendency but the 20W-Ru-IGZO device has a much higher HRS resistance and a smaller set voltage. The I-V curves at HRS state are consisted of

three portions: (1) the Ohmic region with a slope of ~1, (2) the Child law region ($I \propto V^2$) with a slope of ~2, and (3) the region in which the current increases to the compliance current sharply and abruptly, as a trap-controlled space charge limited conduction (SCLC).[29] However, I-V curves of both IGZO and IGZO:Ru devices at LRS states exhibit Ohmic conduction with a linear slope of ~1, which is associated with the formation of conductive filaments. The initial HRS resistances of pure IGZO, 20W-Ru-IGZO and 30W-Ru-IGZO thin films are 1.06×10^8 Ω, 1.63×10^8 Ω and 5.95×10^8 Ω, respectively. That is, the initial HRS resistance is slightly increased owing to Ru doping. In fact, the doped Ru atoms are the defects and, might trap the electron carriers as well as enhance the scattering to the moving electrons. Figure 4(a) shows HRS and LRS resistances of the devices with the compliance currents in the range of 10^{-2}-10^2 mA. As the compliance current increases, both HRS and LRS resistances decrease no matter in pure IGZO devices or in Ru doped ones. The HRS resistances decrease sharply in the reset process and dominate the OFF/ON ratio of the devices. Compared with pure IGZO device, a smaller compliance current and a lower set voltage can switch on the Ru doped devices, as shown in Figures 2(b) and (c). Thus, Ru doping should promote the formation of robust conductive filaments. So higher HRS resistance and consequently higher OFF/ON ratio could be obtained in Ru doped IGZO thin films. On the other hand, too high concentration of doped Ru accelerates the nucleation and formation of tiny and fragile conductive filaments, so the LRS and HRS resistances are increased under a given CC.

Oxygen vacancies in IGZO thin films play a crucial role in carrier transport,[8] and oxygen ions are more mobile than metal cations under an external electric field.[30,31] Hence, the electrochemical migration of oxygen ions and oxygen vacancies should be the main process for the formation and rupture of conductive filaments,[7] and high-resolution XPS has been adopted to measure the oxygen concentration in the pure and 20W-Ru-IGZO thin films. The IGZO (:Ru) thin films are peeled from the interface near the Ag top electrode by Ar^+ plasma gradually, and XPS spectra are measured at each depth. The sample before switching is taken as the initial HRS status, while the samples switched to LRS at a compliance current of 100 mA are taken as the final LRS status for comparison though the 20W-Ru-IGZO device has broken down under this CC. As shown in Figure 4(b), the initial oxygen concentration in the Ru doped thin films is lower than that in pure IGZO films. For both pure and Ru doped IGZO thin films, oxygen concentration is reduced after switched to LRS, namely, the oxygen vacancies are increased in LRS. Furthermore, the oxygen concentration in 20W-Ru-IGZO thin films in LRS under a CC of 100 mA is higher than that in pure IGZO films. Therefore, it is deduced that oxygen vacancies trigger formation/rupture of conductive path when a bias voltage is applied. Simultaneously, it is verified that the formation of conductive filaments becomes easier in Ru doped IGZO thin films since less oxygen vacancies are involved in the process.

Referencing to the above-measured electrical properties and chemical states in the thin films, we proposed the mechanisms for the formation and rupture of

conductive filaments during bipolar switching process, and the enhancement effect by Ru doping can be well understood. For the pure IGZO devices, as shown in Figure 5(a), driven by a positive bias voltage on TE, oxygen ions move toward the Ag anode and are transformed into oxygen gas or be absorbed at the Ag anode[10,32]. Meanwhile, the oxygen vacancies accumulate near the cathode, and the decomposed metals rearrange into the conductive filaments connecting the top and bottom electrodes. As a result, the resistance decreases abruptly and the device is switched into ON state.[7] When a negative bias voltage is applied on the device, the oxygen ions released from Ag/IGZO interface will move back to the IGZO layer and neutralize the oxygen vacancies, resulting in the rupture of conductive filaments, and the device switches back to the OFF state. So the bipolar behavior is essentially a result of the oxidization-reduction of the electrochemically active layer. That is, the formation and rupture of conductive filaments during set/reset cycles mainly take place in a very thin region near the Ag/IGZO interface in the devices. However, under a small CC, the conductive filaments are tiny and fragile because of suppressed bond breakage and oxygen ion migration.[33] When the sweeping voltage is reversed, the filaments will rupture immediately, and the device switches to HRS even before the positive voltage vanishes. Moderate doping of Ru could stabilize the tiny conductive filaments and thus improve the switching characteristics, as shown in Figure 5(b). In essential, the doped Ru might weaken the bonding between metal and oxygen atoms, so it becomes easier for the metal-oxygen bonds to break when a positive bias voltage is applied on the top electrode during the set process. Ru atoms in IGZO matrix participate in the

formation of conductive filaments as well as the accumulation of discontinuous tiny filaments into conductive paths. Furthermore, Ru clusters might enhance the electrical field locally, thus facilitate the formation of robust conductive filaments.[34,35] However, in the IGZO thin films doped with too much Ru, as schematically shown in Figure 5(c), the migration path of oxygen vacancies in IGZO matrix will be shortened and, the nucleation and formation of filaments should be accelerated. Once the tiny filaments are formed, the accumulation of the conductive paths will be suppressed because of the tremendous current along the filaments and the drop of the electrical field. The tiny and fragile filaments result in HRS state even before the positive voltage vanishes, and the BRS characteristics are not tunable by changing CC.

4. Conclusions

In summary, Ru doped IGZO thin films are fabricated by magnetron sputtering and the resistive switching behaviors are studied. Perfect resistive switching characteristics with an OFF/ON ratio of 10^5 were observed under a low compliance current, indicating an excellent performance for the moderate Ru-doped IGZO resistive memory devices. Essentially, appropriate doping of Ru might weaken the bonding interaction between metal and oxygen atoms, facilitate the formation and accumulation of tiny conductive filaments, and enhance the electrical field locally. However, in the thin films doped with excessive Ru, the formation of the metallic filaments becomes more rapid and, tiny and fragile conductive filaments are favorable. In such a case, high resistive state is commonly reached even no negative bias voltage

is applied, resulting in volatile resistive behavior. The small set voltage of 0.5 V and compliance current at a lower level of 10^{-5} A suggest that IGZO doped with Ru of an appropriate concentration is promising for the next generation non-volatile memory.

Acknowledgements

This work was supported by National Natural Science Foundation of China (Grant No. 51071119, 51101081, 51471130, 51271139 and 51271140), Natural Science Foundation of Shaanxi Province (2013JM6002), Fundamental Research Funds for the Central Universities.

References

[1]Y. C. Yang, F. Pan, Q. Liu, M. Liu, and F. Zeng, *Nano Lett.*, 2009, **9**, 1636.

[2] F. Pan, S. Gao, C. Chen, C. Song, F. Zeng, *Mat. Sci. Eng. R*, 2014, **83**, 1.

[3]D. H. Kwon, K. M. Kim, J. H. Jang, J. M. Jeon, M. H. Lee,G. H. Kim, X.-S. Li, G. S. Park, B. Lee, S. Han, M. Kim, and C. S. Hwang, *Nat. Nanotechnol.*, 2010, **5**, 148.

[4]C. B. Lee, B. S. Kang, A. Benayad, M. J. Lee, S.-E. Ahn, K. H. Kim, G. Stefanovich, Y. Park, and I. K. Yoo, *Appl. Phys. Lett.*, 2008, **93**, 042115.

[5]W.-Y. Chang, Y.-C. Lai, T.-B. Wu, S.-F. Wang, F. Chen, and M.-J. Tsai, *Appl. Phys. Lett.*, 2008, **92**, 022110.

[6]Y. S. Lin, F. Zeng, S. G. Tang, H. Y. Liu, C. Chen, S. Gao, Y. G. Wang, and F. Pan, *J. Appl. Phys.*, 2013, **113**, 064510.

[7]C. H. Hsu, Y. S. Fan, and P. T. Liu, *Appl. Phys. Lett.*, 2013, **102**, 062905.

[8]M. S. Kim, Y. H. Hwang, S. Kim, Z. Guo, D. I. Moon, J. M. Choi, M. L. Seol, B. S. Bae, and Y. K. Choi, *Appl. Phys. Lett.*, 2012, **101**, 243503.

[9]Y. H. Kang, T. I. Lee, K. J. Moon, J. Moon, K. Hong, J. H. Cho, W. Lee, and J. M. Myoung, *Mater. Chem. Phys.*, 2013, **138**, 623.

[10]M. C. Chen, T. C. Chang, C. T. Tsai, S. Y. Huang, S. C. Chen, C. W. Hu, S. M. Sze, and M. J. Tsai, *Appl. Phys. Lett.*, 2010, **96**, 262110.

[11]M. J. Lee, S. I. Kim, C. B. Lee, H. Yin, S. E. Ahn, B. S. Kang, K. H. Kim, J. C. Park, C. J. Kim, I. Song, S. W. Kim, G. Stefanovich, J. H. Lee, S. J. Chung, Y. H. Kim, and Y. Park, *Adv. Funct. Mater.*, 2009, **19**, 1587.

[12]Z. Wang, K. Zhao, H. Xu, L. Zhang, J. Ma, and Y. Liu, *Appl. Phys. Express*, 2015, **8**, 014101.

[13]Y. Pei, B. Mai, X. Zhang, R. Hu, Y. Li, Z. Chen, B. Fan, J. Liang, G. Wang, *Curr. Appl. Phys.*, 2015, **15**, 441.

[14]W. Hu, L. Zou, X. Chen, N. Qin, S. Li, and D. Bao, ACS *Appl. Mater. Inter.* 2014, **6**, 5012.

[15]Y.-H. Hwang, H.-M. An, and W.-J. Cho, *Jpn. J. Appl. Phys.*, 2014, **53**, 04EJ04.

[16]R. Waser and M. Aono, Nature Mater. 2007, **6**, 833.

[17]Y. S. Chen, B. Chen, B. Gao, L. F. Liu, X. Y. Liu, and J. F. Kang, *J. Appl. Phys.*, 2013, **113**, 164507.

[18]D. Li, D. Li, C. Zou, *J. Alloy. Compd.*, 2015, **650**, 912.

[19]A. Younis, D. Chu, and S. Li, *RSC Adv.*, 2013, **3**,13422.

[20]T. Tan, T. Guo, Z. Liu, *J. Alloy. Compd.*, 2014, **610**, 388.

[21]L. Chen, H. Y. Gou, Q. Q. Sun, P. Zhou, H. L. Lu, P. F. Wang, S. J. Ding, and D. Zhang, *IEEE Electron Device Lett.*, 2011, **32**, 6.

[22]X. Q. Meng, L. M. Tang and J. B. Li, *J. Phys. Chem. C*, 2010, **114**, 17569.

[23]S. Kumar, P. Kaur, C. L. Chen, R. Thangavel, C. L. Dong, Y. K. Ho, J. F. Lee, T. S. Chan, T. K. Chen, B. H. Mok, S. M. Rao, M. K. Wu, *J. Alloy. Compd.*, 2014, **588**, 705.

[24]D. N. Kim, G. H. Kim, D. L. Kim, S. J. Kim, and H. J. Kim, *Phys. Status Solidi A*, 2010, **207**, 1689.

[25]J. B. Varley, J. R. Weber, A. Janotti, and C. G. Van de Walle, *Appl. Phys. Lett.*, 2010, **97**, 142106.

[26]J.-S. Kim, M.-K. Joo, M. X. Piao, S.-E. Ahn, Y.-Hee. Choi, H.-K. Jang, and G.-T. Kim, *J. Appl. Phys.*, 2014, **115**, 114503.

[27]P. K. Nayak, M. N. Hedhili, D. Cha, and H. N. Alshareef, *Appl. Phys. Lett.*, 2012, **100**, 202106.

[28]J. Chen, L. Wang, X. Su, L. Kong, G. Liu, X. Zhang, *Opt. Express*, 2010, **18**, 1398.

[29]M. A. Lampert, P. Mark, *Current Injection in Solids*; Academic: New York, 1970.

[30]R. Waser, and M. Aono, *Nat. Mater.*, 2007, **6**, 833.

[31]J. Y. Chen, C. L. Hsin, C. W. Huang, C. H. Chiu, Y. T. Huang, S. J. Lin, W. W. Wu, and L. J. Chen, *Nano Lett.*, 2013, **13**, 3671.

[32]J. W. Zhao, J. Sun, H. Q. Huang, F. J. Liu, Z. F. Hu, X. Q. Zhang, *Appl. Surf. Sci.*, 2012, **258**, 4588.

[33]Y. Zhang, H. Q. Wu, Y. Bai, A. Chen, Z. P. Yu, J. Y. Zhang, and H. Qian, *Appl. Phys.*

Lett., 2013, **102**, 233502.

[34]Y. T. Wu, S. Jou, P. J. Yang, *Thin Solid Films*, 2013, **544**, 24.

[35]C. Y. Liu, J. J. Huang, C. H. Lai, *Thin Solid Films*, 2013, **529**, 107.

Figures

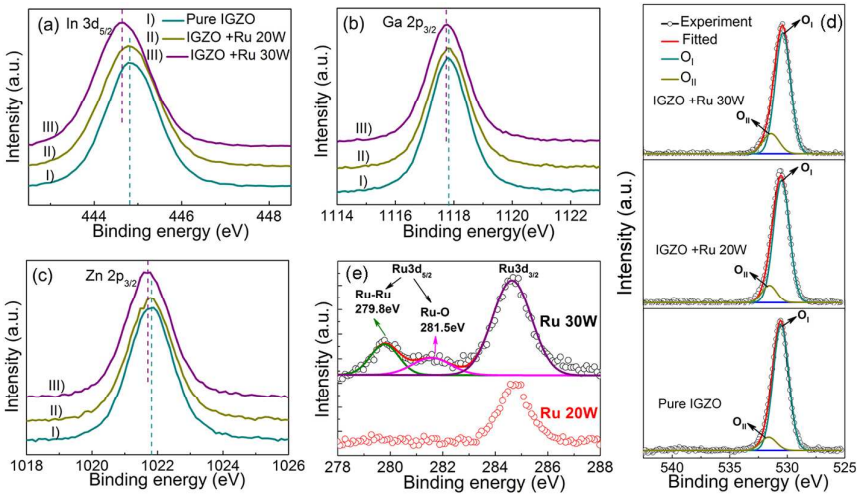

Figure 1 The XPS peaks of In, Ga and Zn in the pure and Ru doped IGZO layers: (a) In; (b) Ga; and (c) Zn; (d) O1s peaks fitted by using a Gaussian profile; (e) XPS peaks of Ru3d in 20W-Ru-IGZO film and fitted XPS peaks of Ru3d in 30W-Ru-IGZO film.

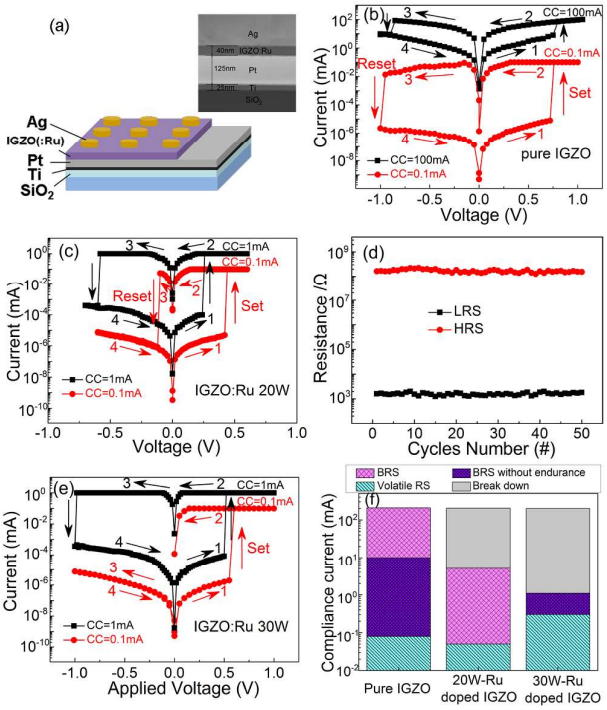

Figure 2 The resistive switching characteristics of pure and Ru doped IGZO devices. (a) Schematic configuration of the Ag/IGZO(:Ru)/Pt device and the inset is the cross-sectional TEM image; (b) I-V curve of pure IGZO device under a CC of 0.1 mA and 100 mA; (c) that of 20W-Ru doped IGZO device under a CC of 0.1 mA and 1mA; (d) Endurance performance of 20W-Ru doped IGZO device under a CC of 0.1 mA; (e) I-V curve of 30W-Ru doped IGZO device under a CC of 0.1 mA and 1 mA; (f) A diagram of the resistive switching behavior as a function of compliance current and Ru concentration.

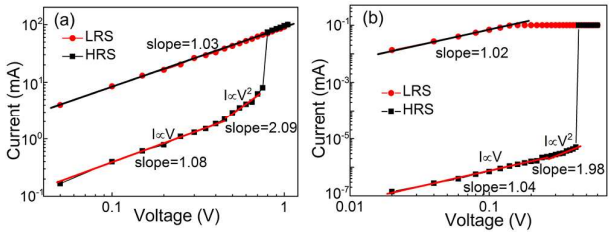

Figure 3 The I-V curves in log-log scale and the fitted slopes for HRS and LRS: (a) pure IGZO and (b) 20W-Ru-IGZO device.

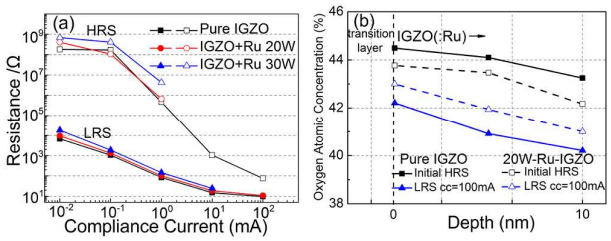

Figure 4 (a) The HRS and LRS resistances of pure IGZO and IGZO:Ru RRAM devices with different compliance currents; (b) XPS depth profiles of oxygen near the interface of Ag top electrode in the pure and 20W-Ru doped IGZO devices at the initial state and at LRS under a CC of 100 mA.

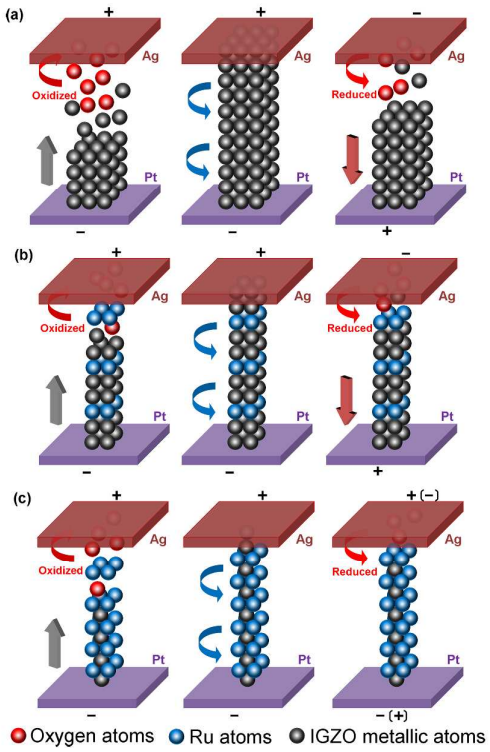

Figure 5 Schematic mechanism for the resistive switching in IGZO-based memory devices of (a) pure IGZO, (b) 20W-Ru-IGZO, and (c) 30W-Ru-IGZO.